Thermodynamics of Metal Ion Binding. 2. Metal Ion Binding by Carbonic Anhydrase Variants†

Charles A. DiTusa,‡ Keith A. McCall,§ Trine Christensen,‡ Mrinal Mahapatro,§ Carol A. Fierke,*,§ and Eric J. Toone*,‡

Department of Chemistry, Duke University, B120 LSRC, Durham, North Carolina 27708, and Department of Chemistry, University of Michigan, Ann Arbor, Michigan 48109

Received July 25, 2000; Revised Manuscript Received November 17, 2000

ABSTRACT: The ability to construct molecular motifs with predictable properties in aqueous solution requires an extensive knowledge of the relationships between structure and energetics. The design of metal binding motifs is currently an area of intense interest in the bioorganic community. To date synthetic motifs designed to bind metal ions lack the remarkable affinities observed in biological systems. To better understand the structural basis of metal ion affinity, we report here the thermodynamics of binding of divalent zinc ions to wild-type and mutant carbonic anhydrases and the interpretation of these parameters in terms of structure. Mutations were made both to the direct His ligand at position 94 and to indirect, or second-shell, ligands Gln-92, Glu-117, and Thr-199. The thermodynamics of ligand binding by several mutant proteins is complicated by the development of a second zinc binding site on mutation; such effects must be considered carefully in the interpretation of thermodynamic data. In all instances modification of the protein produces a complex series of changes in both the enthalpy and entropy of ligand binding. In most cases these effects are most readily rationalized in terms of ligand and protein desolvation, rather than in terms of changes in the direct interactions of ligand and protein. Alteration of second-shell ligands, thought to function primarily by orienting the direct ligands, produces profoundly different effects on the enthalpy of binding, depending on the nature of the residue. These results suggest a range of activities for these ligands, contributing both enthalpic and entropic effects to the overall thermodynamics of binding. Together, our results demonstrate the importance of understanding relationships between structure and hydration in the construction of novel ligands and biological polymers.

Today, efforts to create high-affinity metal binding proteins, either by de novo design or by the redesign of existing scaffolds, represent a major area of activity. Such sites may be used to stabilize proteins, to regulate the activity of proteins, to develop novel catalytic activities, or to create biosensors for the quantification of trace metal ions (*1*−*4*). Because of its high affinity and specificity for zinc, the His_3 metal polyhedron of carbonic anhydrase II (CAII)[1] often has been used as a model for designing metal sites in existing proteins (*5*−*7*), and in de novo-designed proteins such as the minibody (*8*). While metal sites containing 3 or 4 protein ligands and tetrahedral geometry have been successfully prepared, in general these designed metal sites lack the zinc avidity, specificity, and catalytic activity of biological zinc sites, suggesting that structural factors in CAII contribute to the metal affinity and reactivity of this enzyme.

Carbonic anhydrase II (CAII) is a ubiquitous enzyme that catalyzes the hydration of carbon dioxide to carbonic acid (*9*). A catalytic divalent zinc ion is an essential cofactor for this enzyme (*4*). The high-resolution structure (*10*) demonstrates that the catalytic zinc atom is bound near the bottom of a 15 Å conical active site. The picomolar affinity for the zinc ion is afforded by interaction with three histidine imidazole groups, so-called direct ligands, at positions 94, 96, and 119. These ligands are in turn fixed in positions ideal for coordination to the zinc ion by a series of "second-shell" ligands that include Gln-92, Asn-244, and Glu-117. The tetrahedral coordination sphere of zinc is completed by a water molecule, which is hydrogen bonded to Thr-199 (Figure 1).

A crystal structure of CAII has been determined to 1.54 Å resolution, providing an extraordinary level of detail regarding the positions of the interacting atoms (*10*). Structures of a range of mutants have also been determined, as have native protein bound to several metal ions. Although these structures contain within them the structural basis of affinity, extracting this insight from the large number of contacts that provide no contribution to the overall stabiliza-

† This work was supported by the National Institutes of Health (Grant GM57179 to E.J.T. and Grant GM40602 to C.A.F.); C.A.D. and K.A.M. were supported in part by the NIH Pharmacological Sciences and Chemistry-Biology Interface Training Grants, respectively. T.C. was supported by the Danish Research Agency (Grant 9900516) and by the Alfred Benzon Foundation.

* To whom correspondence should be addressed. C.A.F.: phone, (734) 936-2678; fax, (734) 647-4865; e-mail, fierke@umich.edu. E.J.T.: phone, (919) 681-3484; fax, (919) 660-1591; e-mail, toone@chem.duke.edu.

‡ Duke University.

§ University of Michigan.

[1] Abbreviations: CAII, human carbonic anhydrase II; ACES, *N*-(acetamido)-2-aminoethanesulfonic acid; EDTA, (ethylenedinitrilo)-tetraacetic acid; DPA, dipicolinate; Tris, tris(hydroxymethyl)aminomethane; PAR, 4-(2-pyridylazo)resorcinol; CD, circular dichroism; WT, wild-type.

10.1021/bi0017327 CCC: $20.00
Published on Web 04/11/2001

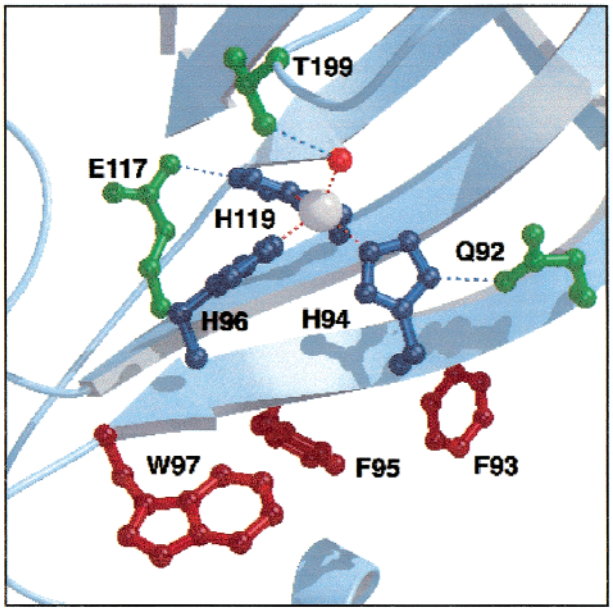

FIGURE 1: Zinc binding site of CAII. Direct metal coordination interactions are indicated by red dashed lines, and indirect (or second-shell) interactions are indicated by blue dashed lines. Zinc-bound hydroxide ion appears as a small red sphere.

tion energy of the complex—or perhaps even contribute unfavorably—is difficult without the corresponding energetic data. Here, we continue our studies of the metal binding properties of carbonic anhydrase as a model metal binding protein. Specifically, we report the calorimetrically determined thermodynamic properties for the binding of metals to mutant proteins. These data, in conjunction with existing structural data, help define the aspects of molecular structure responsible for both affinity and specificity in ligand binding processes.

MATERIALS AND METHODS

Expression and Purification of CAII Variants. The CAII variants were previously prepared by oligonucleotide-directed mutagenesis of the cloned human CAII gene in pCAM (*11*−*13*). The plasmids encoding CAII variants were transformed into *Escherichia coli* strain BL21(DE3) (*14*, *15*). CAII was induced and purified as described (*11*, *16*, *17*). The concentration of CAII was determined by stoichiometric titration with acetazolamide (*17*, *18*).

Preparation of Apoenzyme. In preparing apoenzyme, special care was taken to limit exposure of the protein to metal ions. All buffers and solutions were prepared using deionized water and stored in plasticware previously treated with a 5 mM ethylenediamminetetraacetic acid (EDTA) solution to remove trace metal ions. Metal-free apo-CAII was prepared using Amicon diaflow filtration, washing first against 50 mM dipicolinate (DPA, Sigma or Acros), pH 7.0, and then against 10 mM ACES, pH 7.0. Excess DPA was removed by gel filtration chromatography on a Pharmacia Sephadex PD-10 column (*19*). The residual zinc concentration after apo-preparation was determined using the colorimetric 4-(2-pyridylazo)resorcinol method (*20*, *21*).

Isothermal Titration Microcalorimetry. All thermodynamic data were collected on either an Omega titration microcalorimeter (MicroCal, Inc., Northampton, MA); details of instrument design and data reduction have been reported previously (*22*). Samples consisted of apoprotein (150−300 μM) in 10 mM ACES (Research Organics), pH 7, with buffer in the reference cell. After cell equilibrium was reached, a 5 mM solution of $ZnSO_4$ (volumetric standard, Aldrich) in the same buffer was injected using one of the following injection schedules: 30 injections, 3 μL volume, 10 s duration, 5 min interval; 20 injections, 4 μL volume, 10 s duration, 7 min interval; 19 injections, 5 μL volume, 15 s duration, 7 min interval. The syringe was stirred at 400 rpm. For ΔC_p determinations, titrations were performed at 15, 25, and 35 °C; the cell temperature varied by <0.3 °C over the course of an experiment. Data analysis was carried out using the ORIGIN software supplied by MicroCal. All binding enthalpies are reported after subtraction of the appropriate enthalpy of ligand dilution.

Circular Dichroism Spectroscopy. The CD spectra were recorded at an enzyme concentration of 5 μM in 10 mM sodium phosphate buffer at 25 or 35 °C on an Aviv 62DS spectropolarimeter. The signal was collected using a 1 nm bandwidth, and the value at each wavelength was averaged for 5 s. In the experiment, the change in the extinction coefficient of the sample is determined as calculated from the difference in the absorbance of light circularly polarized in opposite directions. The absorbance change, $\Delta A = A_l - A_r = (\epsilon_l - \epsilon_r)lc = \Delta\epsilon lc$, where $\Delta\epsilon$ is the molar ellipticity and the subscripts l and r are values measured for left and right polarized light, respectively. All ellipticities are reported in units of degress per square centimeter per decimole. The spectra were corrected for baseline contribution of the buffer before being converted to mean residual ellipticity.

RESULTS AND DISCUSSION

To understand the high metal affinity and specificity of CAII, mutations were prepared in the direct ligand His-94, which decrease metal affinity 10^4−10^7-fold (*13*, *23*), and indirect ligands Gln-92, Glu-117, and Thr-199, which reduce zinc affinity ~10-fold each (*12*, *24*). By examining the properties of these mutants, we sought to (1) better understand the origin of the extraordinarily tight metal binding provided by histidine ligands, (2) explore the energetic importance of the second-shell ligands in preorganizing the binding pocket for zinc, and (3) consider the role of Thr-199 as a significant stabilizing force by forming a hydrogen bond with the zinc-bound water molecule. Together, these features of the CAII structure are proposed to provide a majority of the stabilizing force for metal ion complexation.

Loss of a Hydrogen Bonding Interaction: T199A CAII. The crystal structure of wild-type CAII shows that the hydroxyl oxygen of Thr-199 accepts a hydrogen bond from the zinc-bound water, one of the four direct zinc ligands. A second hydrogen bond is formed between the hydroxyl hydrogen of Thr-199 and a carboxylate oxygen of Glu-106 (*10*). Thr-199 was mutated to an alanine to determine the energetic contribution of this indirect ligand. As has been previously observed for the deletion of other second-shell ligands, the zinc affinity decreases by an order of magnitude on deletion of the Thr hydroxyl moiety (*12*) (Table 1). Crystallographic evaluation of the mutant shows that the overall structure is very similar to that of wild-type protein, although a shift in the position of the zinc-bound water allows Glu-106 to accept a hydrogen bond and assume the role of

Table 1: Summary of All Thermodynamic Parameters Obtained for Metal Ion Binding to CAII Variants[a]

CAII variant	ion	K_H[b] (M^{-1})	$\Delta G°_H$[c] (kcal mol^{-1})	$\Delta H°_H$ (kcal mol^{-1})	$\Delta S°_H$ (eu)	K_L (M^{-1})	$\Delta G°_L$ (kcal mol^{-1})	$\Delta H°_L$ (kcal mol^{-1})	$\Delta S°_L$ (eu)
WT	Zn(II)	$(1.2 \pm 0.2) \times 10^{12}$	-16.4 ± 0.2	-8.6 ± 0.2	25 ± 0.7				
Q92A	Zn(II)	$(5.5 \pm 0.6) \times 10^{10}$	-14.6 ± 0.1	-8.6 ± 0.2	20 ± 0.5	–	–	–	–
T199A	Zn(II)	$(1.7 \pm 0.3) \times 10^{10}$	-13.9 ± 0.1	-14 ± 2	0 ± 2	3×10^5	-7.5 ± 0.3	-3 ± 1	15 ± 4
E117A	Zn(II)	$(2.5 \pm 0.9) \times 10^{10}$	-14.2 ± 0.3	2.0 ± 0.5	54 ± 3	3×10^4	-6 ± 0.5	-10 ± 0.7	-13 ± 0.4
H94Q	Zn(II)	$(1.3 \pm 0.5) \times 10^8$	-11.0 ± 0.3	-8.9 ± 0.3	7 ± 0.2	–	–	–	–
H94N	Zn(II)	$(2.5 \pm 0.9) \times 10^7$	-10.1 ± 0.3	-8.4 ± 0.2	6 ± 0.2	–	–	–	–

[a] Subscripts H and L represent values for the high- and low-affinity sites, respectively. Data were collected in experiments performed at 25 °C with 5.0 mM zinc sulfate and 200−300 μM protein. Parameters were determined using the ORIGIN program with one- or two-site curve fitting. Parameters which are not applicable are represented by dashed lines. [b] Determined from equilibrium dialysis (*12*, *13*, *41*). [c] Calculated from K_D values at 25 °C.

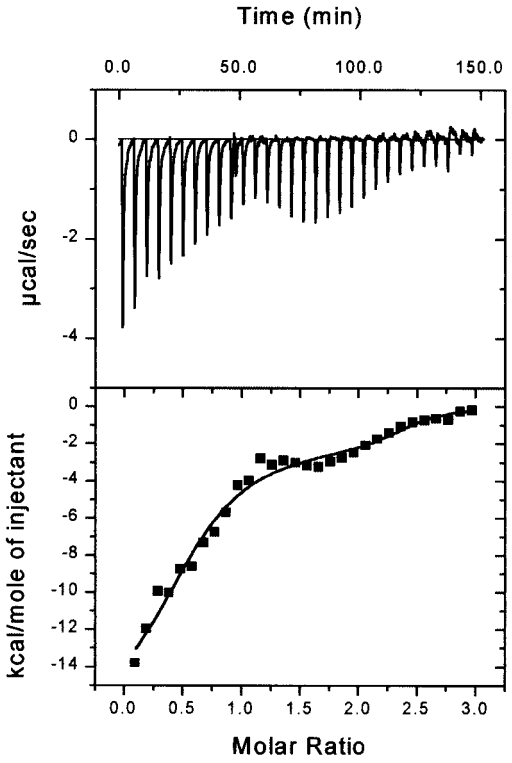

FIGURE 2: Calorimetric titration of zinc sulfate to apo-T199A CAII fit to the two-site binding equation. The concentration of the CAII variant T199A is 299 μM in 10 mM ACES, pH 7, at 25 °C (30 identical injections of 3 μL each of 5.0 mM $ZnSO_4$). The obtained parameters for the high-affinity site are $K = (1.7 \pm 0.3) \times 10^{10}$ M^{-1} and $\Delta H = -14 \pm 2$ kcal mol^{-1}. The obtained parameters for the low-affinity site are $K = 3 \times 10^5$ M^{-1} and $\Delta H = -3 \pm 1$ kcal mol^{-1}.

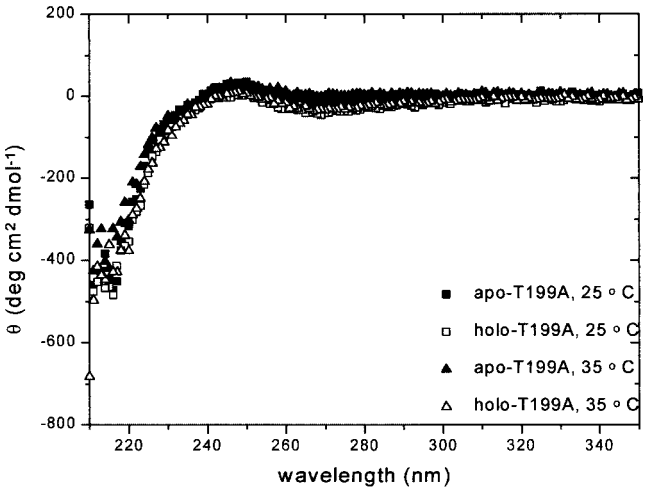

FIGURE 3: Circular dichroism spectrum of apo-T199A CAII superimposed over the spectrum of holo-T199A. Spectra were recorded at 25 and 35 °C at 5 μM T199A variant in 10 mM sodium phosphate buffer. The overlap illustrates that the folded structures of both forms are similar.

indirect ligand. A water molecule not present in the wild-type binding pocket fills the space created by the side chain deletion (*25*). However, the properties of the T199A variant are quite similar to those of T199V CAII, a variant where structure demonstrates that the zinc-bound water forms a hydrogen bond with a solvent molecule (*26*).

A representative thermogram for the titration of apo-T199A CAII with $ZnSO_4$ is shown in the top panel of Figure 2. The bottom panel shows heat evolved per mole of titrant as a function of the molar ratio of total ligand to total enzyme (q_i/X_{tot} vs X_{tot}/M_{tot}). The T199A CAII binding curves are not well described by a single-site binding model but are best fit by a two-site binding equation, assuming a model of independent, i.e., noninteracting, sites (Figure 2). For binding at the tight binding site, the product of the binding constant and the concentration of binding sites, the so-called *c* value (*22*), exceeds 1000, so the reported binding constant and derived free energy of binding were determined by equilibrium dialysis (*24*). The affinity of the second binding site is decreased by almost 5 orders of magnitude compared to that of the first binding site and was determined from the fit to these calorimetric titration data. This second binding is not observed during binding of zinc by wild-type protein (*17*); apparently the deletion of the methyl and hydroxyl moieties at position 199 expands the size of the binding site to the point where two Zn(II) ions fit within the confines of the site. Potentially, the second zinc site could be similar to an inhibitory zinc site identified crystallographically in carboxypeptidase A, where the second zinc ion coordinates a zinc-bound hydroxide and a carboxylate side chain (*27*−*29*). The Thr-199 side chain has previously been identified as important for anion selectivity by discriminating between hydrogen bond donors and acceptors (*30*). Our data suggest that it fulfills a similar function in decreasing the affinity of a second, presumably inhibitory, bound zinc.

To rule out the possibility of large-scale structural reorganization of the protein, circular dichroism spectra of apo- and holo-T199A CAII (one zinc bound) were compared (Figure 3). The defining characteristic of all T199A CAII spectra is the strong negative band at 215 nm, indicative of β-strands. Broad, weak bands are also present centered at 270 nm (negative) and 250 nm (positive). The spectra are temperature independent from 25 to 35 °C. As expected, the

characteristic bands of T199A CAII are all present in CD spectra reported for WT CAII (*31*). The CD spectra of the two proteins are essentially identical, with the apo-T199A CAII spectrum showing no inconsistencies from the holoenzyme spectrum that might indicate a mixture of differently folded enzyme. CD spectra of holo-T199A samples that had not undergone apo-preparation and therefore never had zinc removed from the active site were indistinguishable from the spectra in Figure 3.

To test the validity of the two-zinc model, a 180 μM solution of T199A CAII was treated with 5 mM EDTA for 1 h to ensure that any weakly bound zinc ion was removed. Under these conditions EDTA does not remove zinc from the primary metal binding site. At this point PAR assay showed that the sample contained a 1:1 zinc:enzyme ratio. The EDTA-treated T199A CAII, after removal of the EDTA, was titrated with zinc sulfate, providing a titration curve that was well-described by a one-site binding model with $K_{eq} = (4 \pm 2) \times 10^4$ M^{-1} and $\Delta H° = -6 \pm 2$ kcal mol^{-1}, in reasonable agreement with the values obtained from the two-site fit. The equivalent experiment performed with wild-type protein produced no binding enthalpy up to 0.5 mM zinc sulfate, indicating that removal of the hydoxyl and methyl groups of T199 enhanced the affinity of the second zinc binding site by >40-fold.

Although the free energy of zinc binding by T199A relative to wild-type CAII is reduced by roughly 2 kcal mol^{-1} (Table 1), binding to the mutant protein is significantly more exothermic. In wild-type CAII, Thr-199 hydrogen bonds with and stabilizes a zinc-bound hydroxide ion that ultimately acts as the nucleophilic species in CO_2 hydration. Since the structure of the metal coordination polyhedron is unperturbed in the mutant (*25*), coordination of Zn^{2+} to the histidine imidazoles in T199A CAII presumably proceeds in a fashion essentially identical to that of wild-type protein. The large value of $\Delta H°$ for zinc binding to T199A CAII indicates that metal−histidine coordination is apparently exothermic, proceeding with an enthalpy of binding of at least −14 kcal mol^{-1}. The formation of the hydrogen bond between the zinc-bound water and the hydroxyl group of Thr-199 thus makes an *endothermic* contribution to the overall enthalpy of binding but a *favorable* contribution to the free energy of binding. In addition to enhancing metal affinity, this hydrogen bond lowers the pK_a of the zinc-bound solvent molecule from 8.3 (T199A) to 6.8 (wild-type) (*26*), which decreases the apparent zinc affinity in wild-type CAII since the pK_a of zinc-bound water in a hexaquo zinc complex is 9−10 (*32*, *33*). These effects of the hydrogen bond between the hydroxyl of Thr-199 and zinc-water on the thermodynamics of metal binding almost surely reflect metal desolvation in the CAII·Zn complex, a process predicted to proceed with a large unfavorable enthalpy but a favorable entropy, due in both cases to the liberation of bound water. The entropy increase for releasing a tightly bound water molecule into solution is proposed to have an upper limit of 7 cal M^{-1} K^{-1} (*34*). Therefore, the new water molecule observed in the crystal structure of T199A CAII (*25*) could account for a significant fraction of the difference in binding entropies between wild-type and T199A CAII. This rationalization is consistent with our overall picture of the thermodynamics of metal ion binding being determined largely by metal ion desolvation.

Alteration of Second-Shell Ligands: Gln-92 and Glu-117. The direct histidine ligands of carbonic anhydrase are held in position for interaction with zinc, or preorganized, by second-shell ligands, including Gln-92 and Glu-117 (Figure 1). Mutation of either of these ligands to an alanine decreases zinc affinity about 10-fold, while modestly affecting the catalytic activity of the protein (*12*). The loss of zinc affinity could arise from one or more of three effects: a decrease in the enthalpy of the His−Zn interaction due to reduced electron density on the histidine imidazole, a decrease in the entropy of the unbound state from disruption of the preorganized metal binding site, or changes in the thermodynamics of solvation of the active site.

A zinc titration demonstrates that the enthalpy of zinc binding to Q92A CAII is equivalent to that of wild-type protein near room temperature; therefore, the loss of binding free energy is due entirely to a decrease in the entropy of binding. The unchanged enthalpy of binding could arise in one of two ways. First, the glutamine to alanine substitution could produce no change in either the enthalpy of histidine−zinc interaction or the desolvation enthalpy. Alternatively, this substitution could produce significant but compensating changes in the two processes. Although the functional effect of these two hypotheses is identical—that the $\Delta\Delta G°$ arising from the mutation is attributable to an entropic rather than an enthalpic term—the implications for understanding the molecular features of protein structure relevant to affinity are significant. To distinguish between these possibilities, we next evaluated the change in molar heat capacity accompanying binding; we have previously shown that ΔC_p is exclusively a measure of solvent reorganization (*35*, *36*). The change in molar heat capacity accompanying zinc binding to Q92A CAII is −160 eu, roughly one-third greater than the value of −117 eu we have previously reported for binding to wild-type protein (*17*), suggesting compensating changes in the enthalpy of histidine−zinc interaction and desolvation enthalpy in the mutant. The change in ΔC_p suggests either an *enhanced* contribution from desolvation of nonpolar surface area or a *diminished* contribution from the desolvation of the metal ion to the overall thermodynamics of ligand binding. This latter event seems most likely as the crystal structure demonstrates that the wild-type Q92−H94 hydrogen bond is replaced by a compensatory hydrogen bond formed between the histidine zinc ligand and an inserted water molecule in Q92A CAII (*37*).

Given equivalent enthalpies of binding between wild-type and Q92A CAII, an additional effect must offset the change in the enthalpy of binding arising from differential solvent reorganization. Such effects might include compensating changes in solvation for metal and binding site surface area or differences in the enthalpy of the imidazole−zinc interaction. Although the differential change in molar heat capacity indicates an alteration in the way that the interacting species are desolvated during binding, there is no simple way to relate changes in enthalpy and entropy to these changes. Thus, at this time we can conclude that changes in the solvation properties of the mutant relative to the wild-type protein do contribute to the differential thermodynamics of binding; however, alterations in the enthalpy of the His−Zn interaction and the entropy of preorganization of the metal site may also contribute to the observed changes.

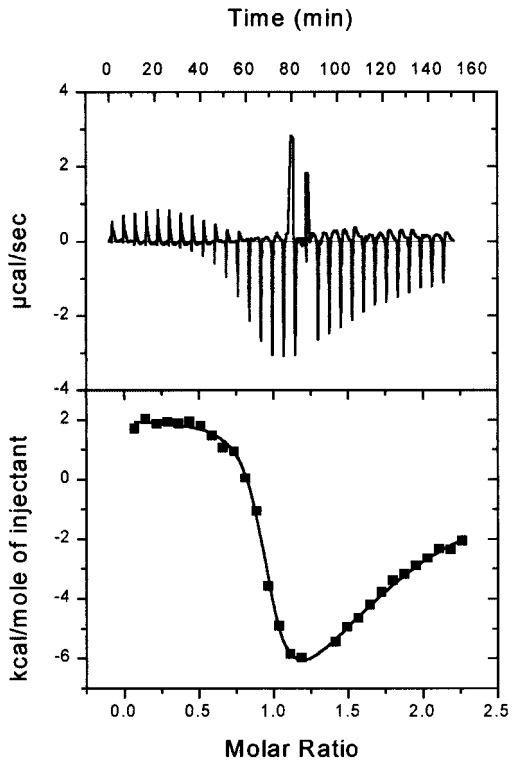

FIGURE 4: Isothermal titration calorimetry curve of zinc binding to apo-E117A CAII fit to the two-site binding equation. The concentration of the E117A CAII variant is 199 μM in 10 mM ACES, pH 7, at 25 °C (30 identical injections of 3 μL each of 5.0 mM $ZnSO_4$). The obtained parameters for the high-affinity site are $K = (2.5 \pm 0.9) \times 10^{10}$ M^{-1} and $\Delta H = 2 \pm 0.5$ kcal mol^{-1}. The obtained parameters for the low-affinity site are $K = 3 \times 10^4$ M^{-1} and $\Delta H = -10 \pm 0.7$ kcal mol^{-1}.

In wild-type CAII, one of the carboxylate oxygens of Glu-117 accepts a hydrogen bond from an imidazole N-H of the direct ligand His-119 (Figure 1); this interaction is postulated to preorganize the binding site and thereby enhance the overall affinity for the active site zinc (*12*). The crystallographically determined structure of E117A CAII is very similar to that of wild-type protein. However, a chloride ion is recruited from solvent to occupy the space vacated by the Glu-117 side chain in E117A (*37*). In addition to decreasing the zinc affinity, removal of the Glu-117−His-119 hydrogen bond significantly enhances the zinc association rate constant. These data have led to a proposed mechanism for zinc binding that involves an initial complex formed by zinc coordination to His-94 and His-96, followed by slow ligand exchange between His-119 and a zinc-bound solvent molecule to form the tetrahedral zinc site (*12*).

A representative titration of E117A CAII with $ZnSO_4$ is shown in Figure 4; the derived thermodynamic properties are listed in Table 1. Again, the mutation results in the formation of a second, weak zinc binding site. The high-resolution crystal structure demonstrates that the space created in the E117A binding site by the deletion of the Glu side chain can accommodate an ion as large as bromide (*37*), a species with a significantly larger ionic radius than Zn(II). The second zinc ion may bind in this same area, located toward the bottom of the binding cleft. The binding of zinc to the low-affinity site of E117A ($K_L = 3 \times 10^4$ M^{-1}) is 10-fold weaker than to the low-affinity site of T199A ($K_L = 3 \times 10^5$ M^{-1}), but is associated with a larger enthalpy of binding. These data suggest that the second-shell ligands may function to both enhance the high-affinity zinc site and to discourage the potentially inhibitory binding of additional zinc ions.

The second striking feature of zinc binding to E117A CAII is that association of zinc in the high-affinity site proceeds with an unfavorable change in enthalpy near room temperature. This thermodynamic pattern is not uncommon in metal ion binding. Thus, for example, binding of Mg^{2+} to various mononucleotides and $tRNA^{Phe}$ is dominated by a large positive entropy change (*38*, *39*). The favorable entropy in these cases is attributed to release of waters strongly bound to fully solvated Mg(II). Although zinc desolvation occurs upon binding to all variants, the entropic effect of water liberation is large—as much as 7 eu per water (*34*)—so small changes in the precise arrangement of water molecules following binding will have large effects on the binding thermodynamics. Here, the change in the thermodynamic parameters of binding could result from several effects, including changes in the thermodynamics of desolvation of the metal ion or the binding site (i.e., the methyl group of the alanine side chain vs the carboxylate of the glutamate side chain), or changes in the interactions of the side chains with each other or with the bound zinc. The observed thermodynamic data for E117A CAII are in significant contrast to those obtained for removal of the second-shell hydrogen bond in Q92A where no change in $\Delta H°$ is observed, suggesting, perhaps, a much larger enthalpic role for the charged glutamate residue as a second-shell ligand than the uncharged glutamine. In the absence of data that facilitate the isolation of solvation-associated thermodynamic effects from those attributable to solute−solute interaction, assignation of bulk thermodynamic properties to specific molecular events is not feasible. Nonetheless, all of the suggested phenomena likely contribute to the overall net enthalpy of metal ion binding.

Modification of "Direct" Ligands: H94N and H94Q CAII. In wild-type CAII, the imidazole nitrogen of His-94 acts as one of the direct ligands of zinc (Figure 1). In place of the histidine imidazole, the carbonyl groups of Asn and Gln side chains can directly coordinate the metal ion with optimal stereochemistry. However, zinc affinity decreases, and in some cases, the metal geometry is altered (*13*).

A representative titration of H94N CAII with zinc sulfate, shown in Figure 5, is consistent with a single zinc binding site. The thermodynamic parameters obtained for zinc binding to the two direct ligand variants are presented in Table 1, along with those of wild-type CAII. Zinc binding constants could not be determined calorimetrically, as the titration curves for both H94N and H94Q CAII exhibited the stepwise behavior expected of high-affinity binding ($c > 1000$, $K > 10^7$ M^{-1}). Therefore, the values of both K_{eq} and the derived free energies reported in Table 1 are from equilibrium dialysis studies.

Remarkably, enthalpies of zinc binding for the direct ligand variants H94N and H94Q are essentially equivalent to that of WT CAII, despite the decreased free energy for zinc binding. As discussed before, a variety of compensating effects likely contribute to the observed phenomenology. Crystal structures of H94N CAII have been determined at 2.0 Å resolution bound both to a molecule of Tris buffer and to the inhibitor acetazolamide (*13*). In the acetazolamide-

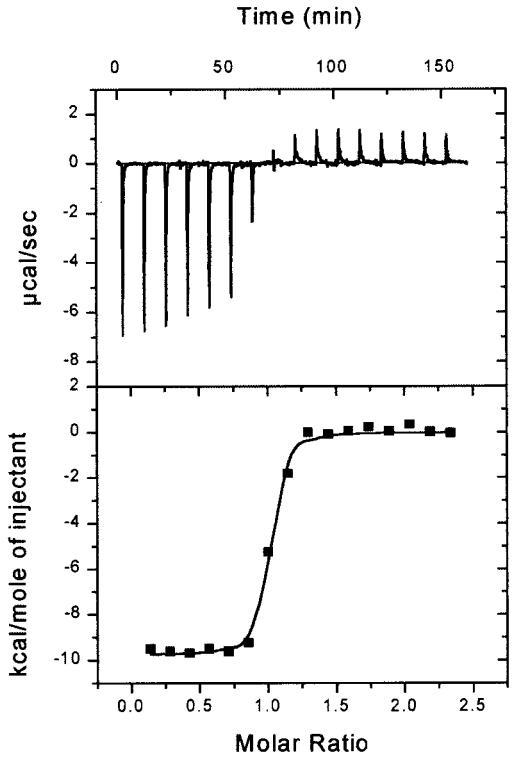

FIGURE 5: Isothermal titration calorimetry curve of Zn(II) binding to apo-H94N CAII fit to the single-site binding equation. The concentration of the H94N CAII variant is 290 μM in 10 mM ACES, pH 7, at 25 °C (30 identical injections of 3 μL each of 5.0 mM $ZnSO_4$). The obtained parameters are $K = (2.5 \pm 0.9) \times 10^7$ M^{-1} and $\Delta H = -8.4 \pm 0.2$ kcal mol^{-1}.

bound structure, a hydrogen bond is observed between Asn-94 and Gln-92, the putative indirect ligand for His-94. In the Tris structure, a minor shift in the position of the asparagine side chain results in an additional hydrogen bond with a Tris oxygen, while the hydrogen bond between the direct and indirect ligands is maintained. Furthermore, the bound metal moves 0.8 Å toward the shorter Asn side chain at position 94, and the geometry changes to trigonal bipyramidal. The crystal structure of H94Q CAII has not been determined, but the glutamine side chain is almost certainly too long to maintain a hydrogen bond to the Q92 side chain. Although the substitution of asparagine or glutamine for histidine at position 94 decreases the free energy for zinc binding, the net binding enthalpy is not decreased, despite the presumably weaker electrostatic interaction of the carbonyl moiety with the metal (*40*). On the other hand, alterations in the position of the bound metal ion and the metal binding geometry result in incomplete desolvation of the bound zinc ion, providing an increase in the favorable enthalpy of binding and a decrease in the entropic effect due to water liberation relative to WT CAII.

An additional source of unfavorable entropy arises from loss of conformational degrees of freedom in amino acid side chains during binding. Zinc binding to asparagine or glutamine freezes out a larger number of degrees of freedom than does binding to histidine in the wild-type protein. The unfavorable $\Delta S°$ upon binding per loss of rotation about one methylene unit is estimated to be 0.5−1.5 eu, suggesting that the unfavorable contribution to $\Delta S°_{conf}$ during binding to H94Q CAII should be larger than that during binding to either H94N or wild-type protein. While this pattern is observed for binding zinc to H94Q relative to wild type, the observed entropy change is nearly identical to that produced during binding of H94N CAII. Apparently differences in solvation again compensate for the effect or flexibility is retained in the bound side chain.

In summary, single amino substitutions in the metal ion binding site of carbonic anhydrase drastically affect the overall thermodynamic parameters associated with metal binding: from a metal site that is apparently purely enthalpically driven (T199A CAII) to a site that is apparently entropically driven (E117A CAII). These overall thermodynamic parameters can be attributed to a variety of intermolecular interactions. In particular, the entropic effect of water liberation is large as the hexaquo zinc ion binds to CAII is accompanied by the release of five coordinated water molecules. The effect of so-called second-shell ligands on binding thermodynamics is large and variable, suggesting that different ligands might play different roles, including orientation of direct ligands and electrostatic effects transmitted through the histidine imidazole. Additionally, small changes in the precise arrangement of water molecules following binding will have large effects on the binding thermodynamics. These studies highlight the difficulty in designing metal binding sites with high affinity and emphasize the need for high-resolution energetic data to provide a context in which to interpret structural data.

ACKNOWLEDGMENT

Wes gratefully acknowledge the assistance of Professor David Christianson and David Cox in preparing Figure 1.

REFERENCES

1. Helinga, H. W. (1998) *Folding Des. 3*, R1−R8.
2. Helinga, H. W., and Marvin, J. S. (1998) *Trends Biotechnol. 16*, 183−189.
3. Regan, L. (1995) *Trends Biochem. Sci. 20*, 280−285.
4. Christianson, D. W., and Fierke, C. A. (1996) *Acc. Chem. Res. 29*, 331−339.
5. Klemba, M., Gardner, K. H., Marino, S., Clarke, N. D., and Regan, L. (1995) *Nat. Struct. Biol. 2*, 368−373.
6. Tainer, J. A., Roberts, V. A., and Getzoff, E. D. (1992) *Curr. Opin. Biotechnol. 3*, 378−387.
7. Schmidt, A. M., Müller, H. N., and Skerra, A. (1996) *Chem. Biol. 3*, 645−653.
8. Pessi, A., Bianchi, E., Crameri, A., Venturini, S., Tramontano, A., and Sollazo, M. (1993) *Nature 362*, 367−369.
9. Lindskog, S. (1997) *Pharmacol. Ther. 74*, 1−20.
10. Håkansson, K., Carlsson, M., Svensson, L. A., and Liljas, A. (1992) *J. Mol. Biol. 227*, 1192−1204.
11. Krebs, J. F., and Fierke, C. A. (1993) *J. Biol. Chem. 268*, 948−954.
12. Kiefer, L. L., Paterno, S. A., and Fierke, C. A. (1995) *J. Am. Chem. Soc. 117*, 6831−6837.
13. Lesburg, C. A., Huang, C.-c., Christianson, D. W., and Fierke, C. A. (1997) *Biochemistry 36*, 15780−15791.
14. Hanahan, D. (1983) *J. Biol. Chem. 166*, 557−580.
15. Studier, F. W., Rosenberg, A. H., Dunn, J. J., and Dubendorf, J. W. (1990) *Methods Enzymol. 185*, 60−89.
16. Nair, S. K., Calderone, T. L., Christianson, D. W., and Fierke, C. A. (1991) *J. Biol. Chem. 266*, 17320−17325.
17. DiTusa, C. A., Christensen, T., McCall, K. A., Fierke, C. A., and Toone, E. J. (2001) *Biochemistry 40*, 5338−5344.
18. Nair, S. K., Krebs, J. F., Christianson, D. W., and Fierke, C. A. (1995) *Biochemistry 34*, 3981−3989.
19. Alexander, R. S., Kiefer, L. L., Fierke, C. A., and Christianson, D. W. (1993) *Biochemistry 32*, 1510−1518.

20. Hunt, J. B., Neece, S. H., Schachman, H. K., and Ginsberg, A. (1984) *J. Biol. Chem. 259*, 14793−14803.
21. McCall, K. A., and Fierke, C. A. (2000) *Anal. Biochem.* (in press).
22. Wiseman, T., Williston, S., Brands, J. F., and Lin, L.-N. (1989) *Anal. Biochem. 179*, 131−137.
23. Kiefer, L. L., and Fierke, C. A. (1994) *Biochemistry 33*, 15233.
24. Kiefer, L. L., Krebs, J. F., Paterno, S. A., and Fierke, C. A. (1993) *Biochemistry 32*, 9896−9900.
25. Xue, Y., Lijas, A., and Jonsson, B.-H. (1993) *Proteins: Struct., Funct., Genet. 17*, 93−106.
26. Krebs, J. F., Ippolito, J. A., Christianson, D. W., and Fierke, C. A. (1993) *J. Biol. Chem. 268*, 27458−27466.
27. Bukrinsky, J. T., Bjerrum, M. J., and Kadziola, A. (1998) *Biochemistry 37*, 16555−16564.
28. Gomez-Ortiz, M., Gomis-Ruth, F. X., Huber, R., and Aviles, F. X. (1997) *FEBS Lett. 400*, 336−340.
29. Larsen, K. S., and Auld, D. S. (1991) *Biochemistry 30*, 2613−2618.
30. Liljas, A., Hakansson, K., Jonsson, B. H., and Xue, Y. (1994) *Eur. J. Biochem. 219*, 1−10.
31. Borén, K., Freskgård, P.-O., and Carlsson, U. (1996) *Protein Sci. 5*, 2479−2484.
32. Sillen, L. G. (1964) *Stability Constants of Metal Ion Complexes*, Vol. 209, 2nd ed., The Chemical Society, London.
33. Lindskog, S., and Nyman, P. O. (1964) *Biochim. Biophys. Acta 85*, 462−474.
34. Dunitz, J. D. (1994) *Science 264*, 670.
35. Oas, T. G., and Toone, E. J. (1997) *Adv. Biophys. Chem. 6*, 1−52.
36. Chervenak, M. C., and Toone, E. J. (1994) *J. Am. Chem. Soc. 116*, 10533−10539.
37. Lesburg, C. A., and Christianson, D. W. (1995) *J. Am. Chem. Soc. 117*, 6838−6844.
38. Rialdi, G., Levy, J., and Biltonen, R. (1972) *Biochemistry 11*, 2472−2479.
39. Beliac, J. P., and Sari, J. C. (1969) *Proc. Natl. Acad. Sci. U.S.A. 64*, 763.
40. Gurd, F. R. N., and Wilcox, P. E. (1956) *Adv. Protein Chem. 11*, 311−428.
41. Hunt, J. A., Ahmed, M., and Fierke, C. A. (1999) *Biochemistry 38*, 9054−9062.

BI0017327